CHAPTER 7

ACOUSTIC EMISSION (AE) ANALYSIS OF ELEVATED TEMPERATURE SCRATCH TEST ON 45S5 BIOGLASS

The previous chapter concludes that the lower traction forces during the scratch test because of the increased temperature suggest that brittle materials can be machined more easily at higher temperatures. As a result, when the material was scratched at a higher temperature, the hardness and critical load decreased. The objective of this chapter is to support the previous studies done in this thesis. It is not a stand-alone study. This provides a qualitative study in support of the previous study. In this chapter, the effect of temperature on AE signals and the scratch depth on different AE signals has been studied.

7.1 Operating parameters

The ramp loading was selected during the tests with the starting load at 20 N with a loading rate of 0.2 N/mm. The scratch stroke length was kept to 5 mm. The scratch speeds are taken as 0.5 mm/s, 1.0 mm/s and 2.0 mm/s. The offset distance between two consecutive scratches was 1 mm. The projected scratch conditions are shown in Table 7.1.

Table 7.1:Projected scratch conditions

Temp. (°C)	Load Type	Load Range (N)	Start Load (N)	End Load (N)	Loading Rate (N/mm)	Stroke (mm)	Scratch Speed (mm/s)	Scratch Offset (mm)
27	Ramp	20-200	20	21	0.2	5	0.5	1
210							1	
420							2	

7.2 Experimental procedure

There are nine scratches made at different temperatures and scratch speeds while other parameters are kept constant. There are three repetitions for every scratch condition. The

AE response is recorded for every scratch. The best scratch response has been considered for further analysis. The samples have been polished to a high degree of surface finish range, 0.1164 μm - 0.1478 μm in terms of R_a. The elucidated experiments are done with the specimen temperature maintained at room temperature (27 ℃), 210 ℃ and 420 ℃. The projected temperature of the sample surface has been monitored through the IR thermometer and controlled through the heat controller of the multipurpose portable heating setup. The AE signals are recorded throughout every scratch condition.

7.3 Results and discussion

Wavelet analysis is an undertowing method for acoustic analysis in aspects of material removal processes[77]. However, its mathematical evolution was staged by Joseph Fourier in the nineteenth century. Fourier transform (FT) is a useful and great signal processing tool for transforming a signal from the time domain to the frequency domain. The definition of Fourier transform implies that a signal f(t) can be decomposed into a family of complex sinusoids $e^{j\omega t}$ as basis functions and the coefficients F(jω) represent the amplitudes of complex sinusoids $e^{j\omega t}$ in the signal f(t). Therefore, the Fourier transform of the signal f(t) is defined as following [78]:

$$\mathrm{F}(j\omega) = \int_{-\infty}^{\infty} f(t) e^{-j\omega t} \mathrm{dt} \qquad (7.1)$$

The major limitation of the Fourier transformation is the inherent compromise that exists between frequency and time resolution. The length of Fourier transformation used can be critical in ensuring that subtle changes in frequency over time [79]. To overcome this deficit short-time Fourier transform (STFT) is developed, which is a sequence of Fourier transforms of a windowed signal. The standard Fourier transform provides the frequency information averaged over the entire signal time interval while the short-time Fourier transform (STFT) provides the time-localized frequency information for situations in

which frequency components of a signal vary over time [80]. However, the precision of the short-time Fourier transform is still limited and is greatly dependent on the size of the window [78].

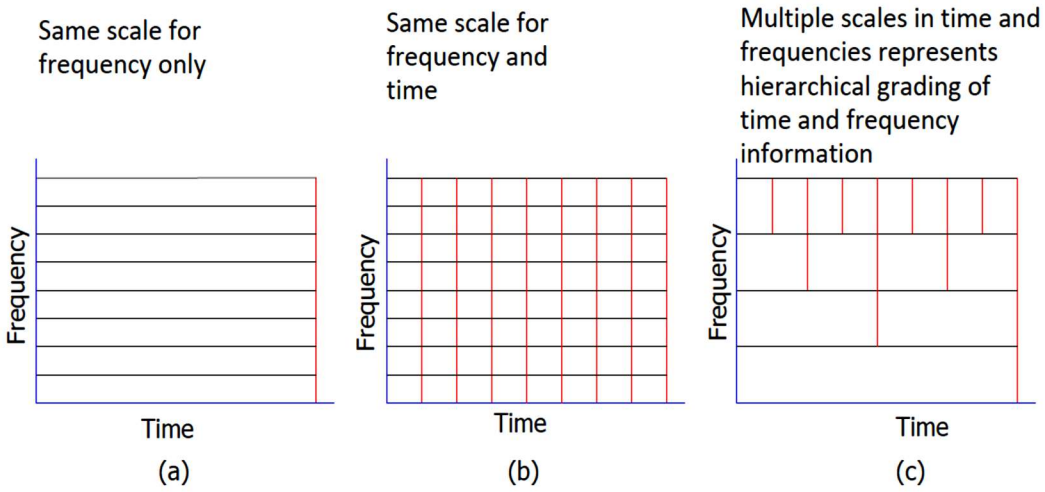

Figure 7.1: (a) Fourier Transform, (b) Short Time Fourier Transform, (c) Wavelet Transform

Wavelet transform offers a generalization of STFT. From a signal theory point of view, like FT and STFT, wavelet transform can be viewed as the projection of a signal into a set of basic functions named wavelets. Such basis functions offer localization in the frequency domain. In contrast to STFT having equally spaced time-frequency localization, wavelet transform provides high-frequency resolution at low frequencies and high time resolution at high frequencies. Figure 7.1 provides a tiling depiction of the time-frequency resolution of wavelet transform as compared to STFT and DFT [80].

Figure 7.1(a) indicates, that in the Fourier transform we know exactly what the content of the frequency signal is but there is no information about when those signals occurred. The high resolution of frequency but uncertainty of time has motivated us to develop a spectrogram, where time and frequency are equally important i.e., Figure 7.1(b). Here in Figure 7.1(b), STFT may have less time and frequency resolution, but it shows when the

individual frequencies turn on and turn off in time. However, Figure 7.1(c) is wavelet transformation, which is a multi-resolution analysis because it represents multiple scales in time and frequencies. In wavelet analysis, there are hierarchical grading of time and frequency information, which means the low frequency tends to last for a long time and does not change very much over time. As the frequency gets higher, the change in frequency also goes higher. This is the multiscale time-frequency decomposition which we are going to use in this experiment. In this transformation, the time-frequency window has a high-frequency resolution for higher frequencies and a high time resolution for lower frequencies. This is a great advantage over STFT where the window size is fixed for all frequencies [80].

The wavelet transform of the signal f(t) is defined as the sum, over all time, of the signal f(t), multiplied by a scaled and shifted version of the wavelet function ψ(t). The coefficients C (a, b) of the wavelet transform of the signal f(t) can be expressed as [78]:

$$C(a,b) = \int_{-\infty}^{\infty} f(t) \frac{1}{\sqrt{a}} \psi\left(\frac{t-b}{a}\right) dt \qquad (7.2)$$

where a and b are the scaling and shifting parameters in the wavelet transform.

There are two types of wavelet transforms: the continuous wavelet transform (CWT) and the discrete wavelet transform (DWT). Specifically, the DWT provides an efficient tool for signal coding [81]. From various types of continuous and discrete wavelets, the Haar wavelet is the discrete type of wavelet which was first proposed and the first orthonormal wavelet basis is the Haar basis. Haar functions have been introduced by Hungarian mathematician. The orthogonal set of Haar functions is defined as a square wave with a magnitude of ±1 in some interval and zero elsewhere [82].

if the time interval t ϵ [0,1] the Haar wavelet family is:

$$h_i(x) = \begin{cases} 1 & for\ t \in [\tau_1, \tau_2] \\ -1 & for\ t \in [\tau_2, \tau_3 \\ 0 & for\ elsewhere \end{cases} \qquad (7.3)$$

Here the notations are as follows:

$$\tau_1 = \frac{k}{m} \qquad \tau_2 = \frac{k+(1/2)}{m} \qquad \tau_3 = \frac{k+1}{m} \qquad (7.4)$$

The integer m = 2^j, j = 0, 1, …, j, indicates the level of the wavelet; k = 0, 1, …., m-1 is the translation parameter. The integer j determines the maximal level of resolution [83]. Each decomposition level indicates a band of frequency. So, by increasing the number of decomposition levels each band will be narrower which means better frequency resolution. The AE responses for different scratch conditions have been recorded. The recording instrument is equipped with a piezo-electric sensor. The resolution of the recording instrument is 1 x 10^{-7} mV. The frequency of the recording instrument is 10^4 Hz. We have performed decomposition at 2 to 6 levels and recorded the statistical data of every level of decomposition. The Figure 7.2(b) shows typical statistical data at decomposition level 5. It gives mean, median, maximum, minimum, range, standard deviation, median absolute deviation, mean absolute deviation, L1 norm, L2 norm, and max norm. Graphs were plotted for every statistical data taken from the analysis corresponding to the different scratch conditions. However, only standard deviation and mean absolute deviations are found to be useful in performing a comparison-based qualitative analysis of different scratches. Hence, only these two values from the wavelet

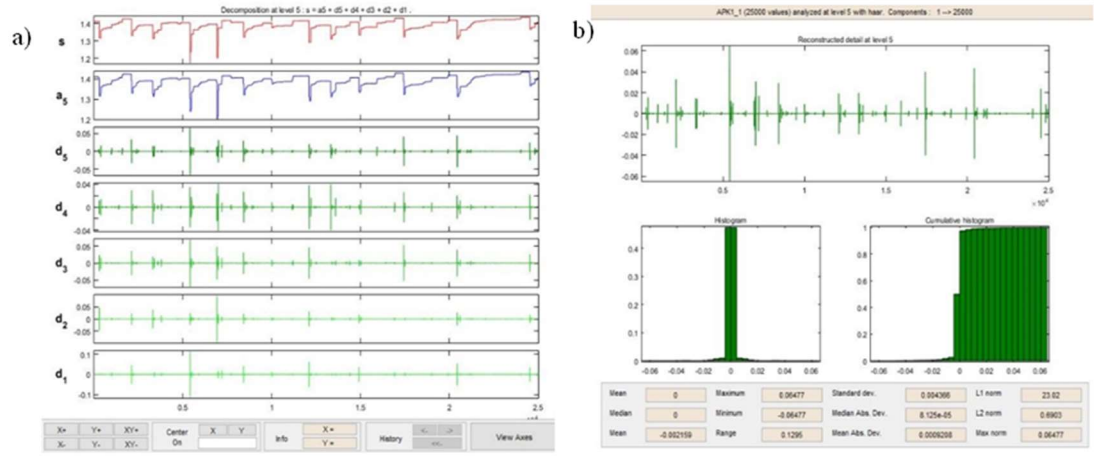

Figure 7.2: Wavelet analysis of acoustic signals; (a) A Typical Examples of wavelet analysis for APK signal for haar wavelet analysis with 5 level decomposition, (b) A typical example of statistical analysis of APK signal at 5th level of decomposition

analysis were chosen for further analysis. It was also observed that only standard deviations and mean absolute deviation values show the repetitive trend but only at 5^{th} level of decomposition and hence are chosen to be used for plotting the qualitative comparisons. For this purpose, a dedicated wavelet design and analysis tool in MATLAB R2015a. There are two types of AE signals recorded during the scratch tests, APK (AE Peak Amplitude) and ASL (Average signal level). As aforementioned, both signals were processed in wavelet design and analysis tool using haar wavelet at 5 levels of decomposition. Furthermore, signal statistical details at the 5th level and the synthesized signal have been considered to perform the comparative analysis at different temperatures and scratch speeds. In this respect, Figure 7.2(a) shows a typical example of wavelet analysis for APK signal for haar wavelet analysis with 5 level decomposition The 's' label shows the original signal, a_5 shows the approximated signal at 5 levels of decomposition. Labels d_5 to d_1 show the increasing frequency band up to 10 kHz. Whereas, the horizontal axis shows the time of the recording. The signal s is the sum of a_5, d_1, d_2, d_3, d_4, and d_5. Figure 7.2(b) shows a typical example of statistical analysis of APK signal at the 5th level of decomposition. The statistical analysis is the insight into the 5^{th} level decomposition. d_5 is the lowest frequency component for the decomposition. It shows that these AE

signals lie in the maximum to minimum with the range of 0.1295 mV. Whereas Table 7.2 shows the standard deviation and mean absolute deviation values for acoustic peak (APK) values for 5th-level decomposition at different temperatures and scratch speeds. After this analysis, Figure 7.3(a) shows a typical example of wavelet analysis for ASL signal for haar wavelet analysis with 5 level decomposition and Figure 7.3(b) shows a typical example of statistical analysis of ASL signal at the 5th level of decomposition. Whereas Table 7.3 shows the standard deviation and mean absolute deviation values for average signal level (ASL) values for 5th-level decomposition at different temperatures and scratch speeds.

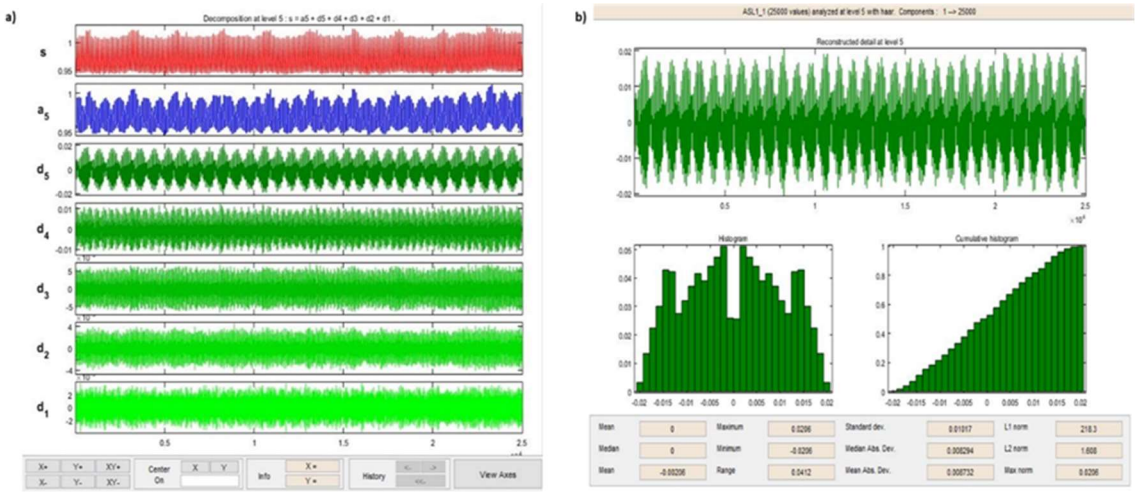

Figure 7.3: Wavelet analysis of acoustic signals; (a) A Typical Examples of wavelet analysis for ASL signal for haar wavelet analysis with 5 level decomposition, (b) A typical example of statistical analysis of ASL signal at 5th level of decomposition

Table 7.2: Standard deviation and mean absolute deviation values for acoustic peak (APK) values for 5th-level decomposition

Temp (°C)↓	**Std. Dev. (mV)**			**Mean Asb. Dev. (mV)**		
Scratch speed (mm/s) →	**2**	**1**	**0.5**	**2**	**1**	**0.5**
27	0.0043660	0.0032600	0.0087200	0.0009208	0.0006514	0.0015920
210	0.0129100	0.0152800	0.0187500	0.0030120	0.0034420	0.0043750
420	0.0147200	0.0136800	0.0174000	0.0024550	0.0028020	0.0038920

Table 7.3: Standard deviation and mean absolute deviation values for average signal level (ASL) values for 5th-level decomposition

Temp (℃)↓	**Std. Dev. (mV)**			**Mean Asb. Dev. (mV)**		
Scratch speed (mm/s) →	**2**	**1**	**0.5**	**2**	**1**	**0.5**
27	0.010170	0.010180	0.016880	0.008732	0.008862	0.014530
210	0.016990	0.016930	0.017170	0.014590	0.014460	0.014790
420	0.021340	0.021100	0.020410	0.019100	0.018450	0.018150

After the statistical analysis, the graphs were plotted to analyze the trend and effect of temperature as well as scratch speed. The Figure 7.4(a) shows plot between the standard deviation and scratch speed for APK values for 5th level of decomposition.,. Figure 7.4(b) shows plot between mean absolute deviation and scratch speed for APK values for 5th level of decomposition, Figure 7.4(c) shows plot between standard deviation of obtained

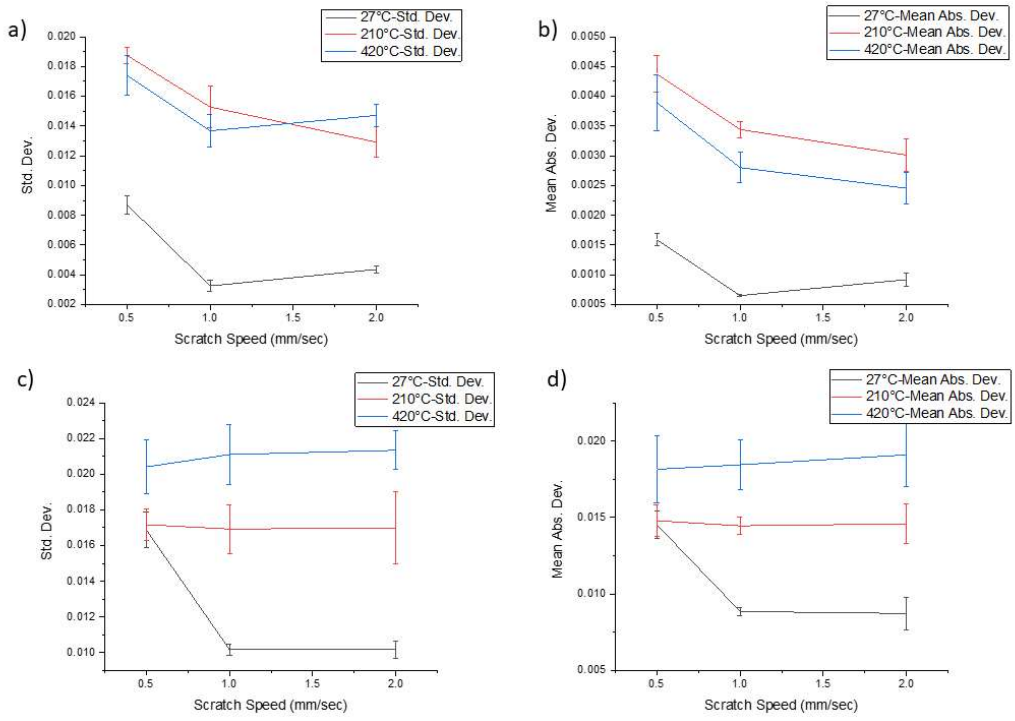

Figure 7.4: AE responses are plotted on different temperatures at 5th level of decomposition; a) Standard deviation versus scratch speed for APK values, b) Mean absolute d deviation versus scratch speed for APK values, c) Standard deviation versus scratch speed for ASL values, and d) Mean absolute d deviation versus scratch speed for ASL values

ASL values for 5th level of decomposition and and scratch speed, and Figure 7.4(d) shows plot between mean absolute deviation and scratch speed for ASL values for 5th level of decomposition. Here, Figure 7.4(a) shows that the standard deviation of the AE signals at increasing temperature keeps on increasing up to 1 mm/s scratch but at higher scratch speed and 210 ℃ shows the decreasing trend. This trend is not so promising to make elucidations for the process. Figure 7.4(b) shows that the mean absolute deviation of AE signals is the highest at 210 ℃ and AE signals are lower at 420 ℃ temperature at different scratch speeds. This trend is again not promising to make process elucidations. Whereas, Figure 7.4(c) and Figure 7.4(d) are found to be in a particular trend. Here, it is seen that the standard deviation and mean absolute deviation of ASL values are higher at high temperatures. Therefore, to confirm this elucidation, the mean values of synthesized signals for APK and ASL are considered for further analysis.

In continuation of the above analysis, the mean values of the synthesized signals have been considered for further analysis. In this respect, Figure 7.5(a) shows a typical example of statistical analysis of synthesized APK signal at 5 levels of decomposition and Figure 7.5(b) shows a typical example of statistical analysis of synthesized ASL signal at 5 levels of decomposition. Whereas, Table 7.4 shows the mean and standard deviation for acoustic peak (APK) values for synthesized signal at 5 level decomposition at different

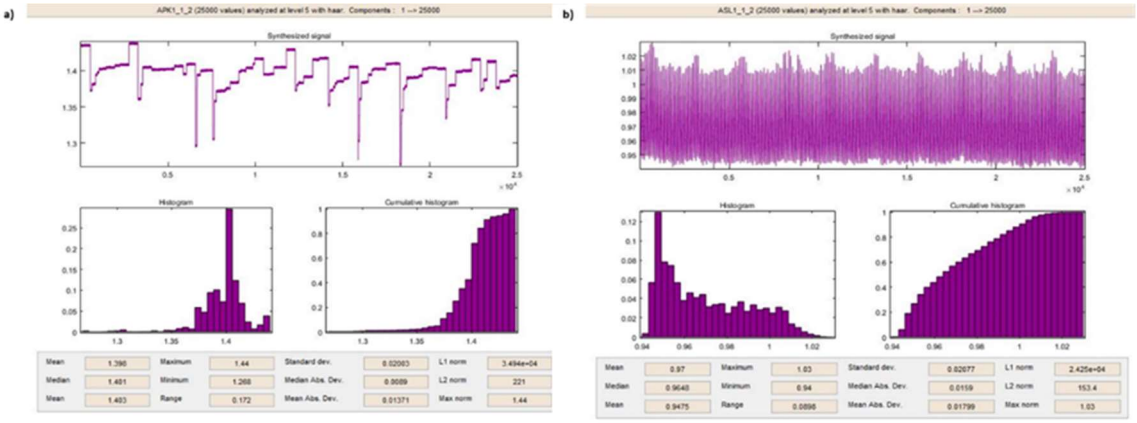

Figure 7.5: (a) A typical example of statistical analysis of synthesized APK signal at 5 levels of decomposition and (b) A typical example of statistical analysis of synthesized ASL signal at 5 levels of decomposition

temperatures and scratch speeds. Table 7.5 shows the mean and standard deviation for average signal level (ASL) values for synthesized signal at 5 level decomposition at different temperatures and scratch speeds.

Table 7.4: The mean and standard deviation for acoustic peak (APK) values for synthesized signal at 5 level decomposition at different temperatures and scratch speeds

Temp (°C)↓	**APK- Mean for synthesized signals (mV)**					
Scratch speed (mm/s) →	**2**		**1**		**0.5**	
	Mean	**Std. Dev.**	**Mean**	**Std. Dev.**	**Mean**	**Std. Dev.**
27	1.39800	0.02003	1.38700	0.02024	1.51300	0.04632
210	1.56800	0.04376	1.59500	0.05353	1.62600	0.06128
420	1.59300	0.04909	1.61500	0.04844	1.65900	0.06188

Table 7.5: The mean and standard deviation for average signal level (ASL) values for synthesized signal at 5 level decomposition at different temperatures and scratch speeds

Temp (°C)↓	**ASL- Mean for synthesized signals (mV)**					
Scratch speed (mm/s) →	**2**		**1**		**0.5**	
	Mean	**Std. Dev.**	**Mean**	**Std. Dev.**	**Mean**	**Std. Dev.**
27	0.97000	0.02077	0.97050	0.02132	0.98460	0.02132
210	0.98650	0.03500	0.98530	0.03461	0.98780	0.03461
420	1.02000	0.04604	1.00700	0.04336	1.02900	0.04336

Based on the above statistical analysis of processed signals, the graphs between scratch speed and mean of APK and ASL values are plotted at different temperatures as shown in Figures 7.6(a) and 7.6(b) respectively. It is observed from Figure 7.6(a) that the mean of APK values is increasing as the increase in temperature at every scratch speed. Subsequently, it is also observed from Figure 7.6(b) that the mean of ASL values is also increasing as the temperature increase at every scratch speed. But, there are large standard errors with mean values. Therefore, this analysis with the processed signal is not correct

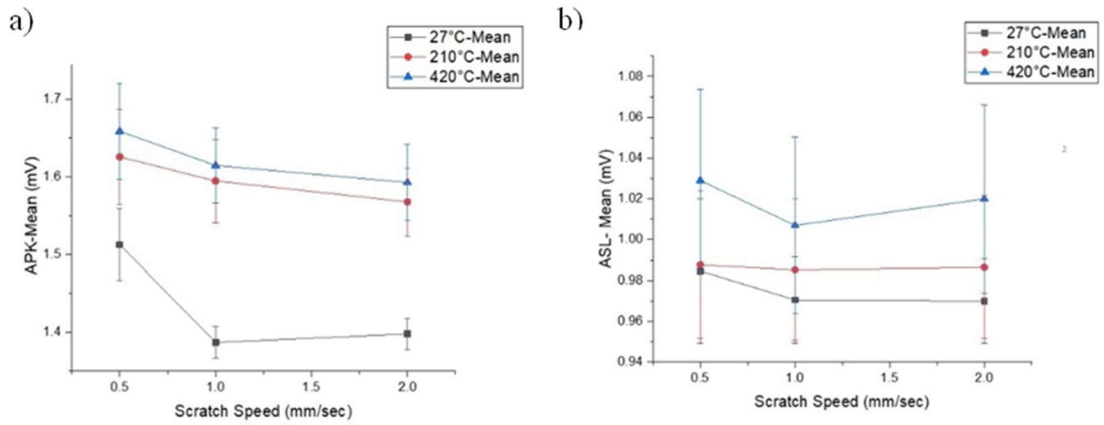

Figure 7.6: AE responses are plotted processed signals on different temperatures at 5th level of decomposition; a) Standard deviation versus scratch speed for APK values, b) Mean absolute d deviation versus scratch speed for APK values

to infer any trend between temperature and mean values of processed signals of APK and

ASL values. The complete results of the wavelet analysis are given in Annexure- III.

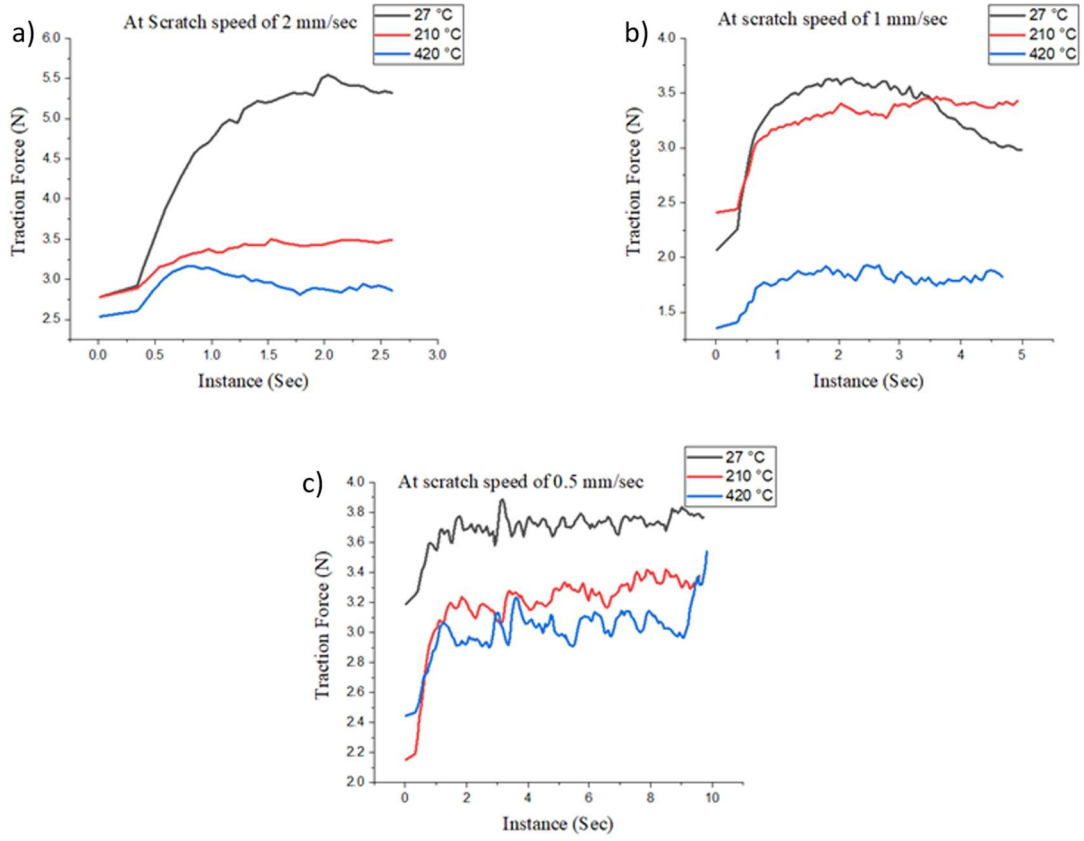

Figure 7.7: Traction forces during scratch tests at different temperatures; a) At scratch speed of 2 mm/s, b) At scratch speed of 1 mm/s and c) At scratch speed of 0.5 mm/s

The AE analysis is done with the 5th level decomposition and processed signals. The APK values are not found suitable for concluding any trend between scratch speed and temperature. Also, the processed ASL signals are not concluding for the same study. Whereas, the ASL values from the 5th level of decomposition, particularly standard deviation and mean absolute deviation are found to be very useful to conclude any trend between scratch speed and temperature.

To identify a proper scratch procedure, the above-mentioned scratches have been compared based on traction load plots and temperatures. For this study, the graphs are plotted between the traction load and instance of time at the temperatures 27 ℃, 210 ℃ and 420 ℃ as shown in Figure 7.7. It is observed from Figures 7.7(a), 7.7(b) and 7.7(c) that there is a significant reduction in traction forces at higher temperatures of samples at every scratch speed which leads to better machinability of ceramic materials. These observations lead to the elucidation that higher temperature led to lower traction forces during scratch. To confirm this elucidation, the SEM images are taken for each condition as shown in Figure 7.8. As the 45S5 bioglass samples are non-conductive, the samples are coated with gold to obtain SEM images. Subsequently, the profile of scratches has been measured with the help of a roughness tester (Surftest, Mitutoyo, SV-2100) to find the depth of cut in the middle of particular scratches. The SEM images lead to the observations that the higher scratch speed up to 2 mm/s leads to crack crack-free surface as well and higher temperature up to 700 ℃ also leads to a higher depth of cut as shown in Figure 7.8. Hence, a higher standard deviation and mean absolute deviation of AE response at 5th level of decomposition also implicate the higher depth of cut.

The SEM images lead to the conclusion that higher scratch speed results in a lateral crack-free scratch as shown in Figure 7.8. It is also observed that higher temperatures lead to more depth of cut and higher MRR. Figure 7.8 shows that the highest depth of cut is 0.568

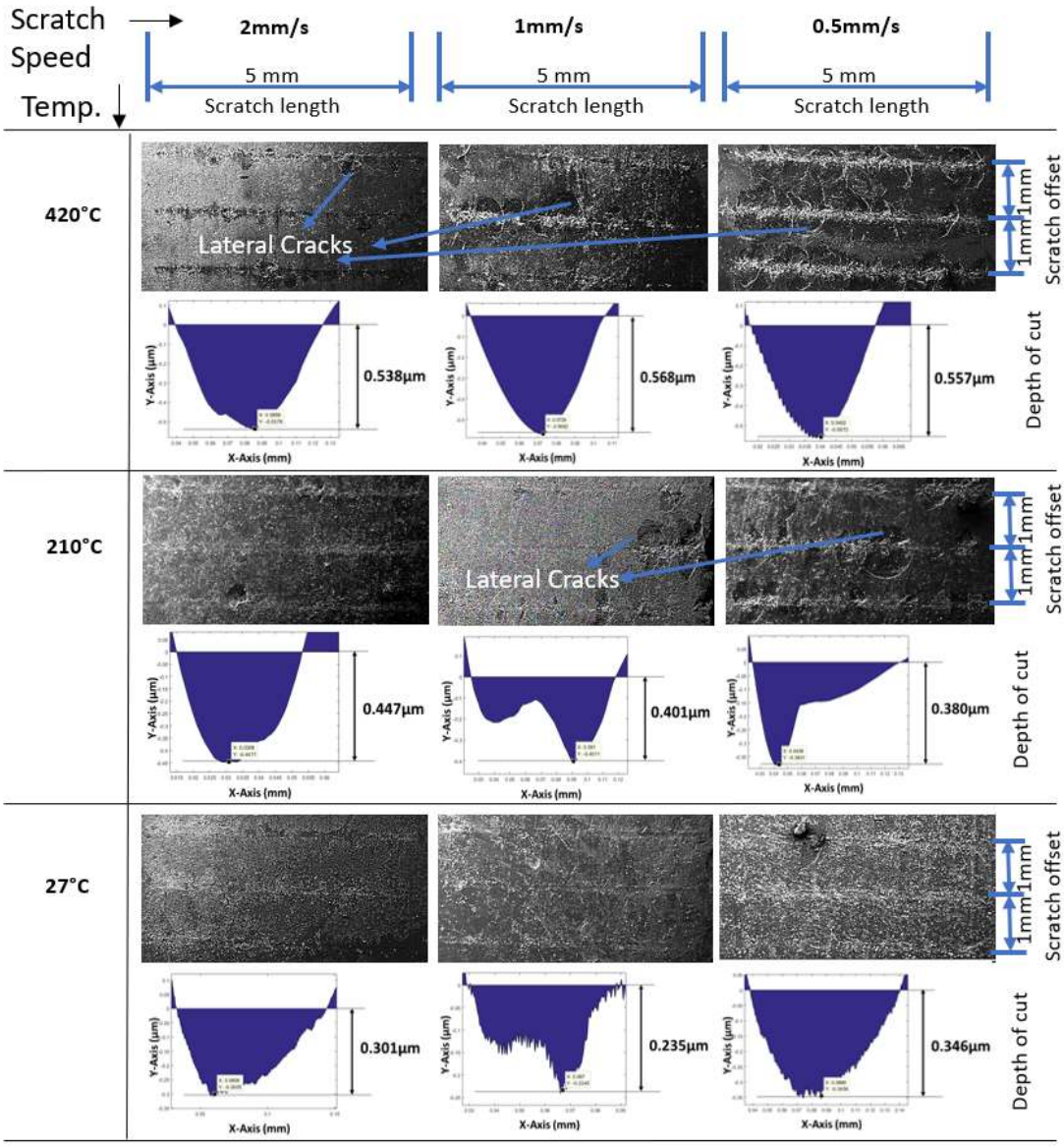

Figure 7.8: SEM images of scratches showing comparison at different temperatures and scratch speeds along with their depth of cuts obtained from contour profile

µm which occurs at 420 ℃ and the lowest depth of cut is 0.235 µm which occurs at 27 ℃. It is also observed from Figure 7.8 that there is no significant effect of scratch speed on the depth of the cut. There are fewer lateral cracks at higher scratch speed which is clearly shown in SEM images. Subsequently, the lateral crack-free scratches represent better machinability which occurs at higher scratch speed. Therefore, this cogitation opens a wide scope for the ductile regime machining of brittle materials. This study also implicates a utilitarian method for machine tool condition monitoring using AE sensors

to achieve better machinability of ceramic materials. This 5-level haar wavelet analysis is easily applicable to AE responses obtained from industrial machine tools performing ductile regime machining operations. Hence, the better machinability range of the mean of processed AE signal as well as ranges of standard deviation and mean absolute deviation are empirically significant for the in-line condition monitoring of machine tools. This method is an uplift to the machinability aspects for 45S5 bioglass as well as other ceramic samples in industries.

7.4 Summary

Nine sets of scratches have been performed on 45S5 bioglass samples at scratch speeds of 2 mm/s, 1 mm/s and 0.5 mm/s as well as sample temperatures 27 °C, 210 °C and 420 °C. The ramp load of 20 - 21 N is applied to the sample with a scratch length of 5 mm. In due course, the AE signals are recorded and 5 level haar wavelet analysis is performed. The standard deviation and mean absolute deviation for APK values for the 5^{th} level of decomposition do not show a continuous trend concerning temperature. Subsequently, it is also found that the standard deviation and mean absolute deviation for ASL values for the 5^{th} level of decomposition show a continuous trend concerning temperature implicating that signal responses are increasing as increase in temperature. On comparing with the traction force plots, SEM images and contour profile of scratches, the higher temperature led to lower traction force and more depth of cut at the same normal loads. In addition to that, the mean values of processed signals for APK and ASL increase with an increase in temperature for APK values as well as ASL values. However, these values can not be used to conclude any trend because of large standard errors. It is found that higher scratch speed results in fewer lateral crack formations at every temperature which represents better machinability. It is convincingly found that the higher scratch speed and higher temperatures lead to ductile regime machining as well as the higher depth of cut

to higher MRR. Therefore, it is a great method to monitor machine tool condition for lateral crack-free scratch as well as ductile regime machining. This study opens up the possibilities for better machinability aspects for 45S5 bioglass and other ceramic samples at high temperatures using an AE sensor and by performing wavelet analysis.